Testing of TAMU3: a Nb_3Sn Block-Coil Dipole with Stress Management

Tim Elliott, Raymond Garrison, Trey Holik, Andrew Jaisle, Alfred McInturff, Peter McIntyre
Accelerator Research Lab, Texas A&M University

Dmytro Abraimov, Van Griffin, and Ashleigh Francis
Applied Superconductivity Center, NHMFL

John Cintorino, Sonny Dimaiuta, Piyush Joshi, Bill Mckeon, & Joe Muratore
Magnet Division, Brookhaven National Laboratory

Maxim Marchevsky
Lawrence Berkeley National Laboratory

Abstract

The Accelerator Research Lab (ARL) at Texas A&M has recently concluded the construction and testing of a superconducting block-coil dipole TAMU3. TAMU3 reached 85% of the resistive-onset short sample critical current (0.1 μV/cm criterion) that was measured on extracted strands at the National High Magnetic Field Lab. Peak magnet current was 6603 amps, and all with quenches originated in the vicinity of the hard-way chicane near the exit lead of the TAMU3c inner winding.

Leading up to the testing we discovered that we had made two grievous mistakes in the fabrication (we mistakenly used the wrong superconducting wire for the cables of the inner windings) and the heat treatment (we used a heat treatment that was too hot and too long). We extracted strands from the leads of the inner and outer windings, and colleagues at NHMFL performed short-sample measurements upon them. The NHMFL measurements indicated RRR ~ 2-5, which gives very little stability against micro-quenches. The short-sample tests of the extracted strands exhibited a long resistive transition, in which there was a current $I_{sc}(B)$ beyond which it became resistive, then a higher current $I_n(B)$ at which it went fully normal. Using the $I_{sc}(B)$ data we predicted a short-sample limit for the revised load line of TAMU3 of 7700 A (9 T) – a disappointing reduction from the 14 T objective.

On those unhappy notes we undertook the testing of the dipole. The first quench occurred at 5695 A, and the dipole trained thereafter to a maximum quench current of 6600 A (7.6 T), 85% of the compromised short-sample limit. All quenches occurred at a single location, in the region of the S-bend transition and outer lead of one inner winding. Data was collected from stress transducers on the outer windings to evaluate stress management, and on the coil ends to evaluate capture of axial forces by static friction lock. The low field reached prevented us from extending those tests to the stress levels where they would have become most interesting, but the designed stress management appeared to be working at the level tested.

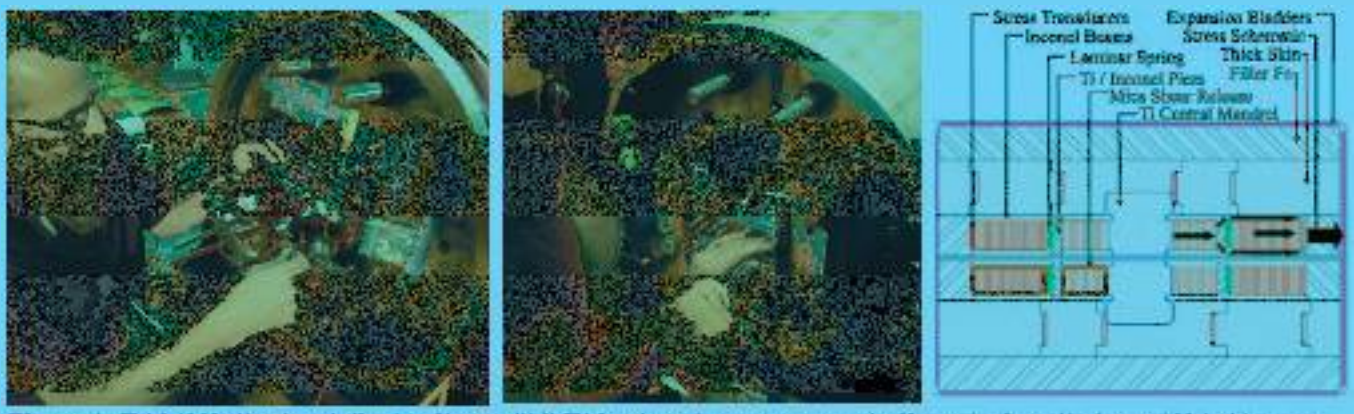


Figure 1. TAMU3 dipole: a) final splices of NbTi leads to interconnect windings; b) installation of Hall bridge sup portive strain gage monitoring the coil ends, c) cross-section showing elements of stress management

TAMU3

The design and fabrication of TAMU 3 dipole has been described previously [1]. Figure 1a shows TAMU3 after assembly of the windings into the flux return and stress shell, with the NbTi interconnect leads spliced to connect the windings. The primary goal of TAMU 3 was to test a method of stress management that intercepts Lorentz force between windings and bypasses stress from inner windings so that the stress in outer windings does not accumulate to a level that could degrade the conductor performance. Figure 1c shows the elements of stress management within the 2-winding coil assemblies. The outer windings were equipped with a set of capacitive stress transducers that measure the stress at the outer boundary of the outer winding.

A second feature of stress management was locking the ends of the windings under static friction to the flux return and stress shell, so that the winding ends are internally captured against axial Lorentz forces. A bridge containing 8 strain gages was assembled onto each end of the flux return (Figure 1b) so that deflections of each of the coil end structures could be measured with respect to the flux return to determine whether they were in fact captured under friction lock.

A system of expansion bladders was located in gaps between the flux return and aluminum stress shell, and on all four sides of the rectangular coil package. The final step of magnet assembly was to heat the entire magnet to ~ 80 C, fill the bladders with low-melt-temp Woods metal, pressurize to 13 MPa, then cool the magnet to freeze the Woods metal and preserve that hydraulic preload through the life of the magnet. The bladder system and preload pressure were designed to provide sufficient preload to keep all elements of the stress management structure closed under full Lorentz load, taking into account differential contraction of all materials to 4 K [1].

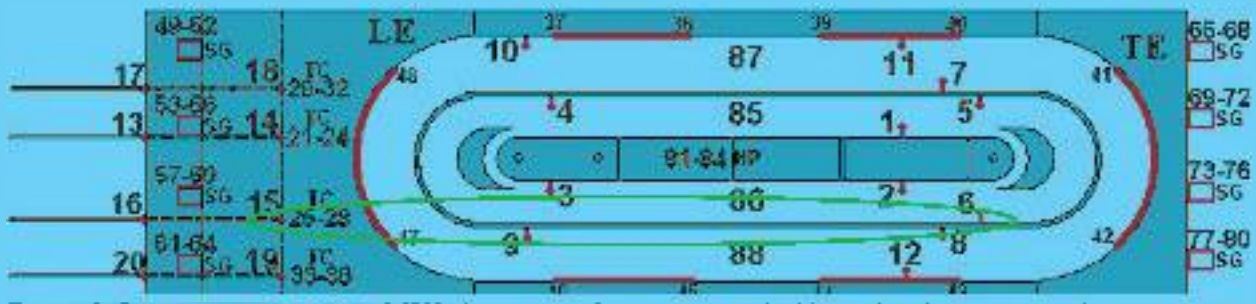


Figure 2. Locations of TAMU3 locations of voltage taps (bold numbers), resistance thermometers (RTD), strain gages (SG), and capacitive stress transducers (small plain numbers). The green oval shows the region in which all quenches occurred.

TAMU3 was instrumented with 3 acoustic sensors that detect the sounds produced when micro-motions occur in the windings or structure or when flux jumps occur among the sub-elements of the superconducting strands. The acoustic sensors were first used in testing HD3 and provide valuable information that complements the voltage signals from voltage taps within the windings [2]. The sensors were attached to the mounting bolts of the H-frame that supports the strain gages (visible in Figure 1b).

TAMU3 was equipped with an array of voltage taps to monitor the voltage drops on segments of each winding. The locations of the voltage taps and resistance thermometers are indicated in Figure 2.

Just weeks before the scheduled tests, we discovered that a mistake had been made in specifying the strand to be used for the cable of the inner windings. It was supposed to be 54/61 RRP wire, instead a spool of long-obsolete MJR wire was used. We had cut-off strands from the leads of each winding, and also witness segments of cable that had been heat-treated along with the windings. Abraimov tested those samples at NHMFL, and the results are summarized in the plots presented below. The RRR was very low, ~2-5, so there was little stability against micro-quench. The transition from superconducting to normal state did not occur abruptly, but over an extended resistive transition (Figure 3b), beginning at current $I_c(B)$ and finally producing a fully normal state at current $I_n(B)$. This data was taken for fields from 7 to 13.5 T, and the onset of resistivity $I_c(B)$ was plotted as a function of field in Figure 3c. The load line for TAMU 3 is shown in Figure 4, as it began in the design, after the mistaken choice of strand for the inner windings, and finally the impact of too-hot, too-long heat treatment. Our 14 T design became a 9 T short-sample-limit dipole as a consequence of those two mistakes.

The signal used to detect quench and to trigger the quench heaters was the difference between the signals across the two entire coil assemblies. This difference signal was chosen to preserve sensitivity to the resistive voltage transient from a quenching domain but suppress power supply transients and other noise that originated outside the magnet. Interestingly the subtraction yielded a ~10% feed-through of power supply noise, which upon investigation we found was due to a slight difference in the inductances of the two coil assemblies. The inductance difference was the result of a slight asymmetry of the gap between coil assembly and steel flux return body. For coil currents >1500 A the difference reduced and disappeared above ~3000 A, which we interpret to be due to the saturation of the nearby steel of the flux return equalizing the inductances.

Voltage differences from each consecutive pairing of voltage taps was pipelined and recorded, both

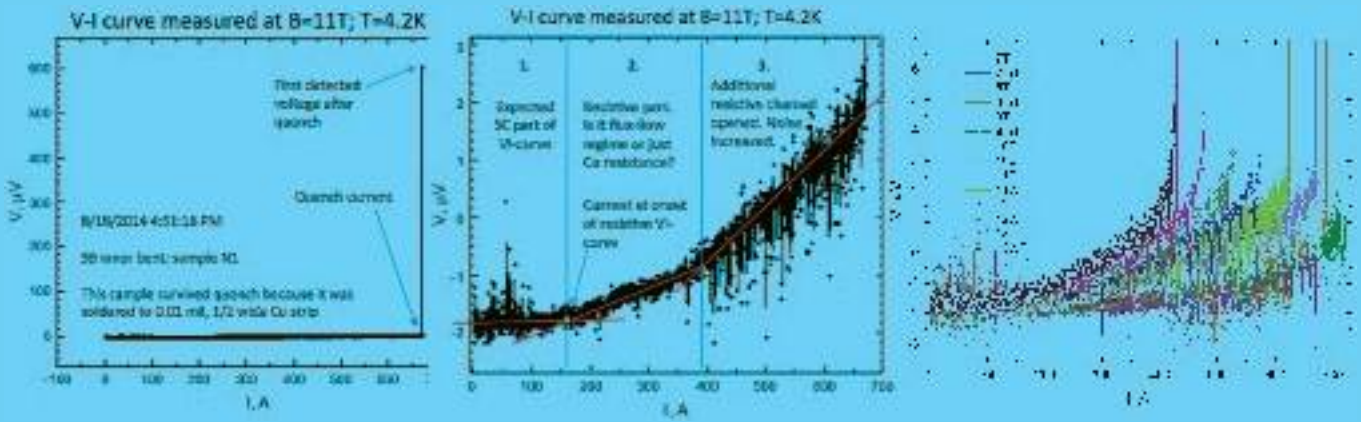


Figure 3. Short-sample measurement of extracted strands of inner windings: a) low-sensitivity superconducting transition, b) same plot with high sensitivity showing resistive transition, c) field dependence of transition.

for a slow continuous record and for fast data during a time interval centered upon the quench detection signal. The signals from a typical quench are shown in Figure 5. The timing of the signal that fired the quench is at t = 0.50 s (that is the selected look-back time for the pipeline record). Saturation of signals was an artifact of the high-gain recording channel that was displayed here to accurately show the startup time of the transient on each tap pair.

The quench originated in the interval between taps 6c and 15c, which corresponds to the outermost half-turn of the inner winding of Coil C as highlighted by the green oval in Figure 2. All quenches occurred in this same location. The quench detection signal fired the quench heaters at t = 0.508 s, which is followed immediately by resistive and inductive transients on all tap pairs in the dipole.

A hall probe from LBNL was used to measure field values and compare to simulation. At 6575 A the calculated absolute magnetic field at the Hall probe location is (5.3 ± 0.2) T, and the measured field was (4.9 ± 0.1) T, presenting reasonable agreement.

Quench origination was detected with 3 acoustic sensors and with traditional voltage detection with a seemingly even distribution of quenches with and without a significant preceding sonic event. Test sequence, Hall probe measurement, carbon resistor thermometry and MIITs, and finally voltage tap and quench origination are discussed below.

Test Summary

I. Tuesday 9/9
   a. At 10 A/s, ramp to 2500 A and stopping every 500 A to collect capacitive transducer data
   b. Controlled Ramp back down
   c. Modifications for following day
      i. Increase sensitivity of Strain gauge data from the mV range to the uV range
      ii. Correct and verify fast and slow logger data labels.

II. Wednesday 9/10
   a. Ramp to 5000 A and stopping every 1000 A to collect capacitive transducer data
   b. Controlled ramp down
   c. Ramp back to 5000 A. During the subsequent ramp the first determined quench occurred at 5630 A
      i. Protection heater induced quench at 5740 A

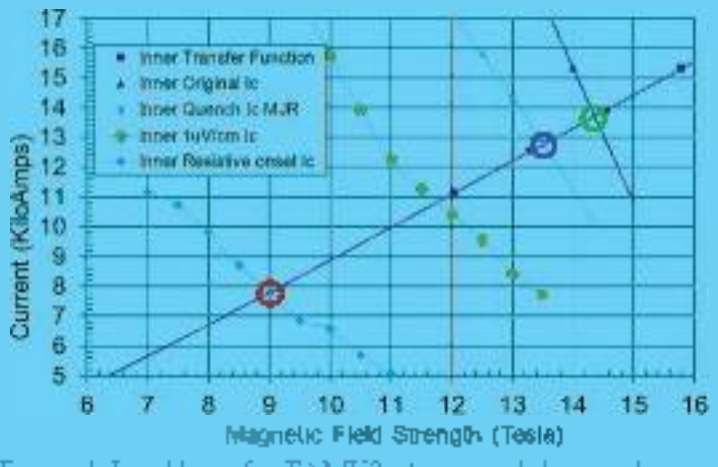


Figure 4 Load lines for TAMU3 as original design. Legend per MJR: the upper or top-bar, non-long-bar treatment

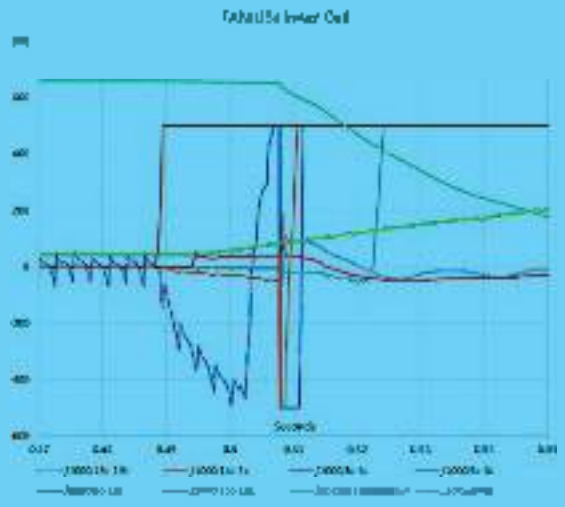


Figure 5 Voltage tap signals from a quench

d. Modifications for following day
    i. Short between DAQ and PS corrected (5740 was the maximum current before the fix)
    ii. Increased Data sampling rate from 1 ms to 0.1 ms
    iii. Added select resistors to fast logger
    iv. Faulty Strain gauge was bypassed by the excitation current source

III. Thursday 9/11
a. First quench at 5695 A
b. We reached 6175 A and collected capacitive transducer data. Reinitiating the ramp induced a quench at 6220 A
c. Reached 5975 A and collected capacitive transducer data. Reinitiating the ramp induced a quench at 6100 A
d. The next two quenches were at 5990 A and 6060 A.
e. Was then determined to perform another protection heater induced quench at 5475 A.

IV. Friday 9/12
a. At 20 A/s the peak current was reached at 6603 A. This equates to a peak field of 7.57 Tesla
b. Subsequent quenches were at 5800 A at 10 A/s, 6300 A at 20 A/s, 6000 at 50 A/s, 5775 A at 100 A/s, and 5710 at 20 A/s.
c. The test was ended at 5:30pm after exhausting all the Helium allotted for the experiment.

Quench Analysis

The transient data shown in Figure 5 can be used to localize the origin of the quench. Since all quenches had exactly the same pattern of voltages, this location was truly the weak point in the entire magnet. Happily we can locate it quite precisely.

The resistive voltage transient occurs in the region between taps 6c and 15c, and then after 0.06 s a transient appears on the voltage between taps 15c and 16c. The temperature is plotted as 10x the actual temperature for clarity. The actual current is 10x larger than that indicated in the chart above.

The above voltage tap trace is indicative of each natural quench that occurred above 5500 A. The voltage between taps 6 and 15 spikes first at roughly 12 ms before the QDC detects quench at the 500 ms mark. This is located between the exit lead splice joint and tail end of the last turn of the TAMU3c inner coil. After 6 ms the quench propagates to the splice joint between voltage taps 15 and 16.

The quench velocity was measured in another quench, shown in Figure 7, in which the resistive transients from the neighboring tap pairs 5 and 6 (in coil assembly TAMU3b) were well-resolved so that a transit time could be measured. The velocity in that case was measured to be at 18.2 m/s at ~3750 A. Since these taps are in the same field region as where the quench originated, and quench velocity is proportional to current density, we can estimate the quench velocity to be 32.1 m/s at 5500 A. This places the quench origination at a location 19.3 cm on the magnet side of voltage tap 15. The quench location is therefore approximately in the middle of the hard way bend of the chicane between the magnet base and the last turn of the inner winding, and is indicated by the blue arrows in Figure 6.

The above localization agrees well with the timing at which the resistance thermometer CR-2 detects a temperature rise at the splice of the outer lead of the inner winding to its NbTi leads. The CR-2 temperature is plotted in Figure 5, and begins a ~linear temperature ramp at t = 0.495 s, corresponding to the heat transfer from a heat source ~20 cm from the end of the splice.



Figure 6. TAMUSc winding showing the location where it is estimated that quench originated.

The dump resistor and protection heaters fire 20 ms after quench was first initiated. The inner coils were quenched between 6 and 8 ms after the protection heater was fired. It is worth noting here that much time and effort was spent in a new insulation scheme [3] coupled to thin layers of Kapton insulation for the protection heaters in order to bring this diffusion time down. This is one of several success stories of the testing of TAMU 3.

The peak quench integral throughout the test was 1.58 MIITs, which corresponds to a peak coil temperature of 58 K. The carbon resistor CR-2 touching the cable at voltage tap 15 measured a single-degree temperature rise at the same time that the quench front reached the same tap. With rudimentary calibration using the Steinhart-Hart model, the peak temperature measured by the resistor was two seconds after the quench at 63 K with an uncertainty of 5 K.

Capacitive Stress Transducer Measurements

Table I presents the measured pressure and calculated pressure from simulation on each capacitive strain gauge is listed below. The calculated pressure is the idealized case assuming that there is zero friction between the windings and the support structure, and that all of the outward Lorentz pressure from the outer windings is measured by the transducer. In reality there is a certain level of cohesion and friction between the windings through the mica paper to the support structure. It is not surprising that the measured pressure is much smaller than the calculated. This small measured pressure is a strong indication that there was no transfer of Lorentz force between the inner winding and the outer winding, and therefore that the stress management structure operated as intended.

While collecting data for transducer #8 we lost data integrity from a likely short between layers of stainless steel. The leads to transducer number 3 were lost internally to the magnet during cool down.

It is worth mentioning that there is a sizable jump in the measured force between 5725 A and 6175 A. This is an indication that the Lorentz force in the outer winding for TAMU 3b and TAMU 3c reaches a

Table 1. Capacitive stress transducer data for two ramps.

	Current = 5775 Amps		Measured		Calculated	
Trace	Transducer	Location	MPa	Uncertainty,	MPa	Uncertainty
	[illegible]	[illegible]	-1	1.1	21.45	1.05
2	A2	Left TE	2.7	1.3	21.80	0.82
3	A3	TE				
4	A4	Right TE	1	1.1	21.47	1.01
5	A5	Right LE	1.1	1.2	21.85	0.88
6	A6	TE	1	1.2	21.57	1.03
7	B1 (TAMUSB)	Left TE	1	1.1	21.45	0.94
8	B2	Left TE				
9	B3	TE	-1	1.1	21.35	1.01
10	B4	Right TE	3.2	1.2	21.80	0.83
11	B5	Right TE	-0.1	1.2	21.45	1.06
12	B6	TE	1.1	1.1	21.77	0.75

	Current = 6176 Amps		Measured		Calculated	
Trace	Transducer	Location	MPa	Uncertainty	MPa	Uncertainty
1	A1 (TAMUSB)	Left LE	4.0	1.3	24.17	0.87
2	A2	Left TE	4	1.4	24.21	0.94
3	A3	TE	Lost lead			
4	A4	Right TE	3.7	1.4	24.21	0.84
5	A5	Right TE	4.1	1.1	24.15	1.02
6	A6	TE	1.1	1.1	24.35	0.96
7	B1 (TAMUSB)	Left LE	0.0	1.1	24.15	0.97
8	B2	Left TE	Zero point calibration lost between shots			
9	B3	TE	3.2	1.2	23.88	0.89
10	B4	Right TE	4.5	1.1	24.24	1.04
11	B5	Right TE	2.3	1.1	24.15	0.97
12	B6	TE	4.7	1.2	23.90	0.88

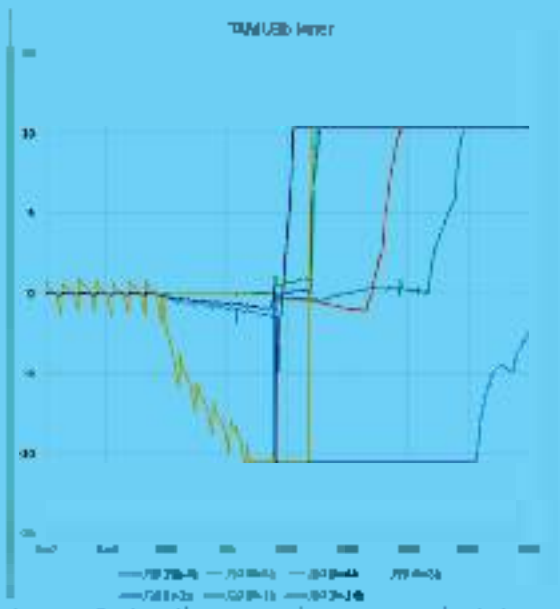


Figure 7. Another quench event in which the transducers in two adjacent top pairs enabled measurement of quench velocity.

level of about 22 MPa at roughly 6000 A, at which the Lorentz force overcomes the static friction between layers of the mica paper and forces transferal of force between the outer winding and the support structure commences. The mica paper has a low coefficient of static friction and releases shear stress at lower applied lateral stress than any other material even under large compressive loading. The mica paper layer was installed on all stress management surfaces to prevent accumulation of shear stress at the boundary, to inhibit sudden 'stick-slip' motion, and to allow for gradual compression of the windings.

Axial Force Analysis

Axial loads in TAMUB were designed to be contained internally within the magnet package and transferred to the flux return by a method of static friction lock. A 7.5 mm thick pair of titanium Surrounds the lead and tail curved sections of the inner and outer windings. Titanium contracts substantially less than the surrounding steel at cryogenic temperatures, and so places the titanium under large compressional loads. The vertical loading is designed to lock the support structure in place by transferring axial forces through static friction to the flux return stress shell assembly. The support structure is also in intimate contact with the coil for supporting the Lorentz force of both the inner and outer windings. Axial strain gauges are strategically located to measure the effectiveness of friction lock.

There were 4 strain gauges located at the end of each coil for a total of 16 gauges measuring axial force transferred through the friction locked stress management structure. During the process of installation and cool down we lost eight on 3 of the 16 gauges. We lost one gauge from TAMUBe lead end, one from TAMUBe tail end, and one from TAMUBb tail end. To compensate for the lost gauges the integrated force from the three working gauges was multiplied by 4/3 and the uncertainty was augmented and is indicated on the following graph. There was no correlation between strain gauge position (left, left middle, right middle, and right) and measured force.

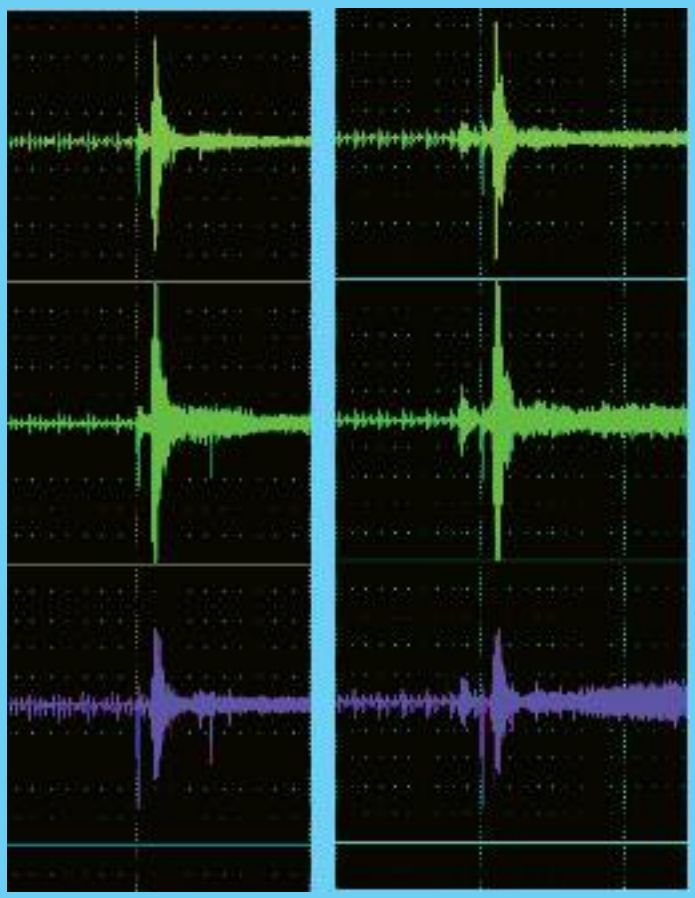


Figure 9. Acoustic signals from two quenches. The time of the quench heater firing is indicated by the vertical dashed line.

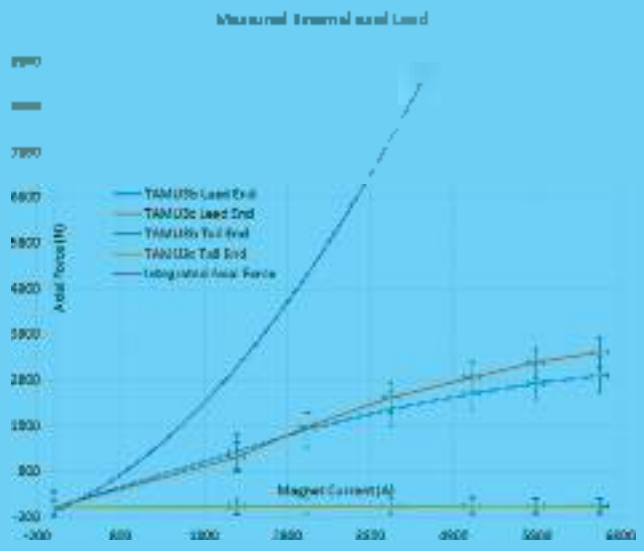


Figure 8. Axial load measured on Le strain gage bridges on each coil end

Throughout the experiment there was no evidence of over-straining any of the strain gages and no significant zero-point shift. The tail end of both coils saw almost zero transfer of axial Lorentz force through the friction lock elements, indicating that the coil end was friction-locked within the flux return per the design.

The lead end strain gauges measured a symmetric axial force transferred through the friction lock and surrounding lead end shoe elements. The measured force (~3000 N at 6000 A) is much less than the integrated axial force as calculated by stress/strain simulations. The lead-end axial force is repeatable (elastic) with succeeding quenches. We interpret this data to indicate that while vertical compression provided friction lock to prevent axial motion on the tail end, the elastic motion on the lead end indicates that there must be no friction lock, and hence no vertical compression. One possible conjecture is that the top-face bladder was filled with molten Woods metal from fittings on the tail end, and it is possible that the Woods metal could have failed to reach the lead end of the bladder interior and therefore to deliver preload. This seems implausible, but it is the only conjecture we have at present. We will investigate this question before and after removing the windings from the flux return during the post-test disassembly.

The force is not quadratic as expected from Lorentz force and predicted by Euler-Bernoulli beam bending but rather is linear. This nearly linear response is an expected result if the support is non-linear in a fashion similar to that of a truck axle leaf-spring. If the tail end were captured under friction lock

and the lead end were not, the entire lead-end section of the coil assembly would be pushed by the axial Lorentz force, and the primary restraining element would be the 'thick-skin' mandrel on which each winding is fabricated. The two end shoes are welded to this thick-skin, and so it would act as a stiff spring to control axial motion. If that conjecture were correct, that tiny axial motion of the lead-end structure would exert tension upon the captured chicane of the 4 leads, and could perhaps explain the reproducible first quench in the outer lead of the inner winding of coil 3c. We will evaluate this carefully when we disassemble the magnet.

Conclusions

TAMU3 produced much valuable information that will continue to be analyzed and employed in the design of subsequent magnets. The instability of the inner conductor for TAMU3 limited the amount of field that TAMU3 was initially designed to reach. The quench in a hard-way bend gives a specific location for the weakest-sister cable. The pattern of transverse and axial forces contains mysteries that we will probe in disassembly and dissection.

The successes of TAMU3 are many. The thin insulation and protection heater design were extremely effective at reducing the diffusion time to <10 ms. The touted capacitive stress transducers were effective at registering forces at substantially lower force values than originally designed. The axial load strain gauge redundancy allowed statistically significant forces to be measured despite the loss of 3 gauges. TAMU3 is one of the few superconducting magnets to date to have sonic transducers be employed for quench analysis. Additionally the MIITS peak temp (58 K) and the localized carbon resistor (63 K) are in good agreement and verify the validity of previous quench calculations [4]. The simulated field (5.35 ± 0.25 T) and the measured field (4.89 ± 0.15 T) were in fair agreement and validated the Vector Fields simulation.

We plan to verify the location of the quench and determine its cause by dissection. TAMU3 will be shipped back to TAMU where the expansion bladders will be deflated and the coils will be uninstalled from the flux return. The questions surrounding apparent absence of friction lock on the lead end and the absence of transverse loading upon the capacitive transducers will be particular targets of investigation. TAMU3c will be autopsied to determine if the quenches were caused by epoxy voids, tin leakage, shorts, broken strands, axial motion, compressive stress in the chicane, lack of rigidity of the titanium element for axial friction lock, mica paper removal of coil cohesion to support structure, or a combination thereof. The face of the windings that abuts the 'thick skin' mandrell will be analyzed to determine the extent of tin leakage on the inaccessible underside of the windings.

References

[1] C. Benson *et al.*, 'Construction and testing of TAMU3, a 14 Tesla stress-managed Nb_3Sn model dipole', Adv. in Cryo. Eng. 57A/B, AIP Conf. Proc. 1434, 649 (2012). http://scitation.aip.org/content/aip/proceeding/aipcp/10.1063/1.4706975

E. Holik *et al.*, 'Current progress of TAMU3: A block coil stress-managed high field (>12T) Nb_3Sn dipole', Proc. Particle Accel. Conf., New York, March 26-April 1, 2011. http://accelconf.web.cern.ch/accelconf/pac2011/papers/tup178.pdf

R. Blackburn *et al.*, 'Fabrication of TAMU3, a wind/react stress-managed 14T Nb_3Sn block coil dipole', 8th Eur. Conf. on Appl. Superconduct. (EUCAS'07): J. of Physics Conf. Series **97**, 012128 (2008). https://accelconf.web.cern.ch/accelconf/PAC2011/papers/tup104.pdf

[2] M. Marchevsky *et al.*, 'Test of the high-field Nb_3Sn dipole magnet HD3b', IEEE Trans. Appl. Superconductivity 24(3) 4002106 (2014). http://ieeexplore.ieee.org/stamp/stamp.jsp?arnumber=6634238

[3] Raymond Blackburn *et al.*, 'Improved S-2 glass fabric insulation for Nb_3Sn Rutherford cable', IEEE Trans. Appl. Superconductivity 18(2)1391 (2008). http://accelconf.web.cern.ch/accelconf/pac2011/papers/tup178.pdf

[4] E. Holik *et al.*, 'Construction challenges and solutions in TAMU3, a 14 T stress-managed Nb_3Sn dipole', Adv. in Cryo. Eng. 1573, 1535, (2014). http://scitation.aip.org/content/aip/proceeding/aipcp/10.1063/1.4860889